Syndiotacticity-Rich Poly(vinyl alcohol) Fibers Spun from *N*-Methylmorpholine-*N*-oxide/Water Mixture

N. NAGASHIMA, S. MATSUZAWA,* and M. OKAZAKI

Faculty of Textile Science and Technology, Shinshu University, 3-15-1 Tokida, Ueda, Nagano 386, Japan

SYNOPSIS

Aqueous NMMO solutions containing NMMO above 50% are good solvents for syndiotacticity-rich poly(vinyl alcohol) (s-PVA). Although water is not a good solvent and dissolves s-PVA at temperatures above 100°C, the mixtures dissolve it at temperatures below 100°C. s-PVA fibers were prepared through gel-spinning of s-PVA/NMMO/water (NMMO : water = 70 : 30) mixtures in cold water and wet-spinning of the solution in methanol. The mechanical properties and fine structure of the drawn fibers were examined based on the results of measurements of tensile properties, thermal properties, birefringence, and optical and electron microscopic observations. The strength and Young's modulus of the drawn fibers were approximately to 2.0 and 45 GPa, respectively. The reason why the fibers with theoretical mechanical properties could not be prepared was surmised to be related to the structure of the amorphous regions. © 1996 John Wiley & Sons, Inc.

INTRODUCTION

High-performance polyethylene (PE) fibers with a Young's modulus of 150 GPa and tensile strength of 3 GPa were prepared through gel spinning by Smith and Lemstra in 1980.[1] However, the fibers have low heat resistance due to the low melting point of around 140°C. Since commercial (atactic) poly(vinyl alcohol) (a-PVA) has a higher melting point of 220°C, the preparation of high-performance a-PVA fibers has been actively studied. A-PVA fibers with the high tensile strength of 2.0–3.0 GPa can be routinely prepared although those with a tensile strength of 6.0 GPa have not yet been prepared. The fibers can be prepared by spinning the solutions containing boric acid followed by heat drawing,[2,3] gel spinning of the ethylene glycol solutions[4] and dimethyl sulfoxide/water solutions followed by heat drawing,[5] and gel spinning of glycerine solutions followed by zone drawing.[6]

High-performance syndiotacticity-rich PVA (s-PVA) fibers with a higher melting point (250°C) than that of a-PVA and hot-water resistance can be prepared by gel spinning of hot dimethyl sulfoxide/water solutions followed by heat drawing[7] and spinning of the hydrochloric acid solutions accompanied by neutralization followed by heat drawing.[8] s-PVA fibers with a tensile strength of 2.0–2.5 GPa can be prepared.

Since water is not a good solvent for s-PVA, aqueous s-PVA solutions easily form gels.[9] Although dimethyl sulfoxide is a better solvent than is water, it is not a good solvent for s-PVA.[10] Hydrochloric acid is a good solvent for s-PVA.[8] However, careful handling is required for its use in acid. *N*-Methylmorpholine-*N*-oxide (NMMO)/water mixtures dissolve cellulose through the breaking of the hydrogen bonds between the hydroxyl groups of cellulose.[11] The NMMO solutions were presumed to be good solvents for s-PVA. This article describes the investigations concerning the dissolution of a- and s-PVAs in the NMMO solutions, the gelatin of the PVA/NMMO/water mixture, the stability of PVA chains in the solution, and the preparation of high-performance s-PVA fibers from the NMMO solutions with an NMMO content above 60% by the

* To whom correspondence should be addressed.

Journal of Applied Polymer Science, Vol. 62, 1551–1559 (1996)
 CCC 0021-8995/96/101551-09

Table I Raw PVAs

Sample	DP	s-diad (%)[a]	Triad (%)[b] S	H	I
a-PVA-1	1700	55.2	30.6	49.2	20.2
a-PVA-2	4000	55.8	31.0	49.6	19.4
s(61)-PVA-1	1640	61.0	36.6	48.7	14.7
s(61)-PVA-2	6830	60.4	35.6	49.6	14.8
s(64)-PVA	1150	63.8	40.8	45.9	13.3

[a] Amounts of syndiotactic diad in samples. s = S + H/2.
[b] S, H, and I are amounts of syndiotactic, heterotactic, and isotactic triads in samples estimated from the NMR spectrum.

gel spinning of the solution into water followed by heat drawing.

EXPERIMENTAL

Materials

The PVAs used are shown in Table I. PVAs except for s(64)-PVA were supplied by Kuraray Co. The s(64)-PVA was derived by the saponification of poly(vinyl trifluoroacetate) obtained through the photopolymerization of vinyl trifluoroacetate at −78°C.[12] NMMO monohydrate with a melting point of 75°C was supplied by Nihon Nyukazai Co. Aqueous NMMO solutions with various concentrations of NMMO were used as solvents.

Dissolution and Gelation Temperature

PVA films were put into test tubes containing NMMO solutions of various concentrations; then, the dissolution temperatures of the PVAs were measured at a heating rate of 3 min/1°C. Sixty milligrams of PVA films cut into 3 × 5 mm pieces was added to 2 mL of the solution to achieve a concentration of 0.03% after dissolution. The critical gelation concentrations of PVA were determined for solutions at different NMMO concentrations at 30, 0, and −34°C based on the immobilization of the solutions when tubes are turned upside down.

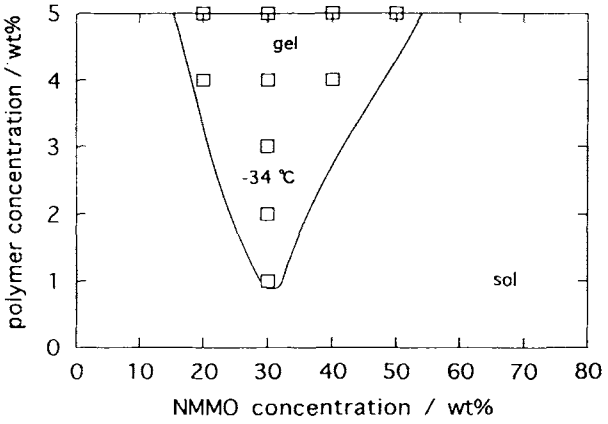

Figure 2 Gelation ability of a-PVA-1.

Viscometry for the Determination of Viscosity Equation and Stability of Solution

Intrinsic viscosities [η] were determined by extrapolating the reduced viscosity to the zero concentration at 100°C for the PVAs with the same tacticity and different degrees of polymerization. The viscosity was measured with an Ostwald viscometer at 100°C because of the high viscosity at 30°C. K and α in the equation $[\eta] = KM^{\alpha}$ for s-PVA were esti-

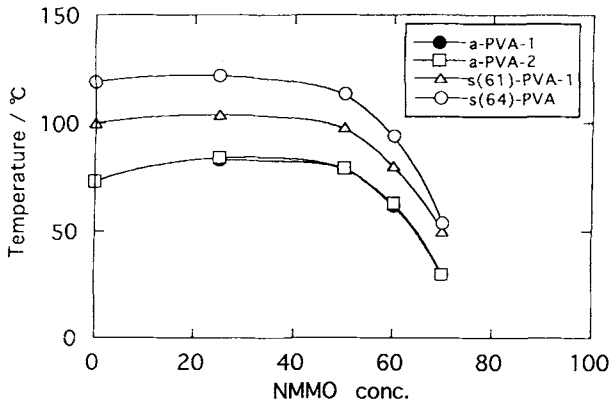

Figure 1 Relationships between dissolving temperature of PVA and NMMO concentration.

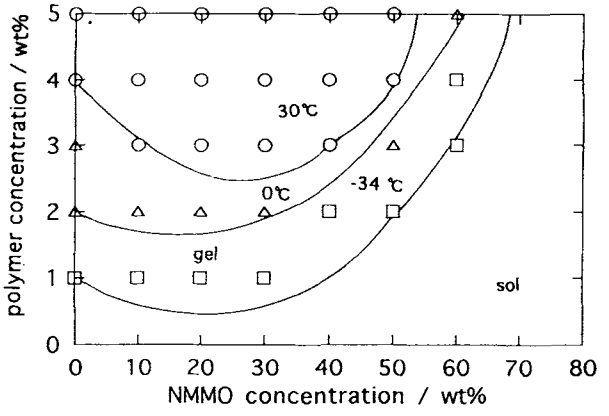

Figure 3 Gelation ability of s(61)-PVA-1: (○) gelation at 30°C; (△) gelation at 0°C; (□) gelation at −34°C.

Table II Intrinsic Viscosities, [η], in NMMO/water mixture and constant α for viscosity equation estimated from [η]

Sample	[η]	α
a-PVA-1	1.01	0.76
a-PVA-2	1.27	
s(61)-PVA-1	0.76	0.75
s(61)-PVA-2	2.23	

mated from [η] of the PVAs with different molecular weights. The solutions were prepared by dissolving PVA in a 70% NMMO solution at 100°C. The stability of the PVA chains in the solution was estimated from the change in viscosity with time in the presence and absence of hydrogen peroxide and oxalic acid.

Spinning

Spinning solutions were prepared by dissolving each PVA in 70% NMMO solutions at 100°C. The PVA concentrations were fixed at 6 and 8%, which were lower than that for the preparation of commercial PVA fibers that led to the decrease in the ratio of entanglement of the polymer chains. The temperature most suitable for spinning was determined from the viscosities of the spinning solutions measured using a Tokyo Keiki HM-8 viscometer in the range of 40–80°C. Spinning solutions kept at 80°C were extruded from a nozzle with a diameter of 0.5 mm into a coagulation bath with a length of 1.2 m by applying a nitrogen gas pressure of 0.35 kgf. Wet spinning caused by coagulation and gel spinning caused by gelation were carried out. Methanol was used for wet spinning, and cold water, for gel spinning as a coagulation bath. Extrudates were washed for 24 h in methanol or water, then dried by fixing on a frame without stretching.

Drawing

Drawing was performed in a hot oven using a hand-operated drawing device. Drawing temperature was controlled at 200 and 220°C with an accuracy of 2°C. Spun filaments with a length of 10 mm were drawn at a draw rate of 1 mm/s.

Tensile Test

The strength and Young's modulus of each fiber were measured in an NMB TOM-5 tensile tester. Gauge length was set at 10 mm. Crosshead speed was 10 mm/min. Each strength and Young's modulus value shown here represents an average of five individual measurements.

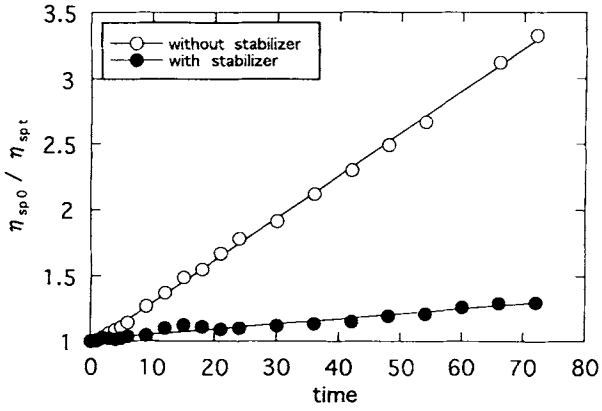

Figure 4 Viscosity changes in s(64)-PVA solution with time (hydrogen peroxide of 0.1% and oxalic acid of 0.1% were added together as stabilizers).

Differential Scanning Calorimetry (DSC)

Thermal analysis was performed using a Mac Science TAPS1000 differential scanning calorimeter. About 1 mg of the fibers was used for each run. DSC curves were obtained in a temperature range of 25–280°C and at a scanning rate of 20°C/min. The melting points of the fibers were taken as the maximum of the melting curves.

Optical Birefringence

Birefringence was measured using a Nihon Bunko polarizing microscope with a Wetzer compensator.

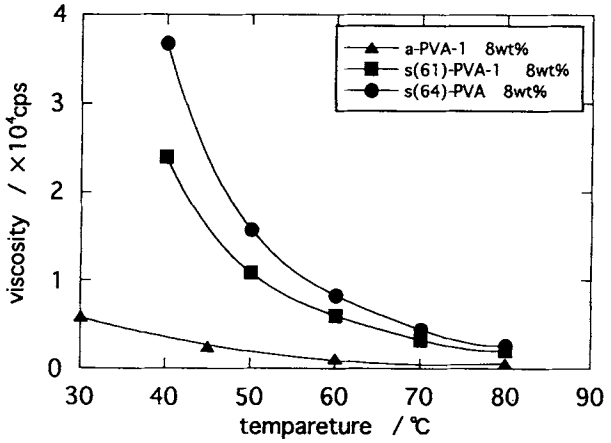

Figure 5 Dependencies of the viscosity of the spinning solutions on temperature.

Table III Spinning Conditions

Sample No.	PVA	Polymer Concentration[a] (wt %)	Coagulation Bath (Temperature)	Results
1-A	s(64)-PVA	6	Water (5°C)	Dispersion
1-B			Methanol (25°C)	Fragile fiber
1-a		8	Water (5°C)	Uniform fiber
1-b			Methanol (25°C)	Uniform fiber
2-A	s(61)-PVA-1	6	Water (5°C)	Dispersion
2-B			Methanol (25°C)	Fragile fiber
2-a		8	Water (5°C)	Dispersion
2-b			Methanol (25°C)	Uniform fiber
3-A	a-PVA-1	6	Water (5°C)	Dispersion
3-B			Methanol (25°C)	Fragile fiber
3-a		8	Water (5°C)	Dispersion
3-b			Methanol (25°C)	Fragile fiber

[a] Solvent; 70% NMMO aqueous solution.

Birefringences were then calculated using the following equation:

$$\frac{(c/10^4) \times 10^4 f_{(i)}}{d_0} = n \times 10^3$$

where $c/10^4$ is a specific number for the compensator; $f_{(i)}$, a constant from $i = (a - b)/2$; and d_0, the diameter of the fibers. The value of $c/10^4 = 2.625$ was used, and the value of a and b were measured values.

Observation with a Microscope

Drawn and undrawn fibers were observed using a Nihon Kougaku OPTIHOL-POL polarizing microscope (POM) and a Nihon Denshi JOEL ASM-T220A scanning electron microscope (SEM). The specimen for SEM observation had been coated with gold.

RESULTS AND DISCUSSION

Figure 1 shows the relationships between the NMMO concentration in aqueous solution and the dissolution temperature of the a- and s-PVAs. The dissolution temperature was nearly equal to that in water for the solutions containing less than 50% NMMO but dropped abruptly in the solutions containing over 50% NMMO. NMMO solutions tended to be good solvents when the NMMO concentration

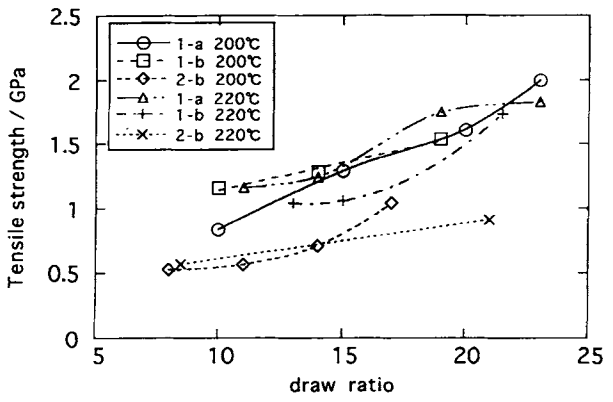

Figure 6 Relationships between tensile strength and draw ratio.

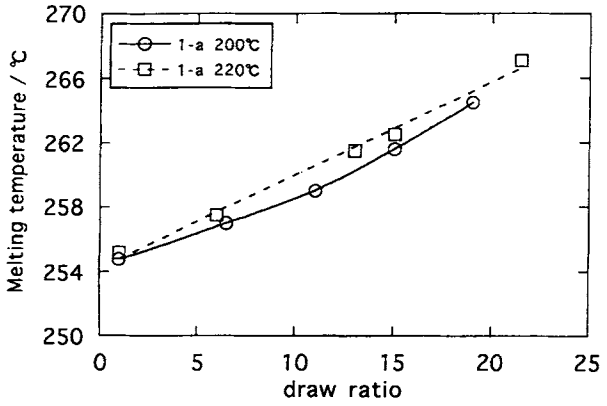

Figure 7 Relationship between melting point of gel-spun fiber and draw ratio: (○) drawing at 200°C; (□) drawing at 220°C.

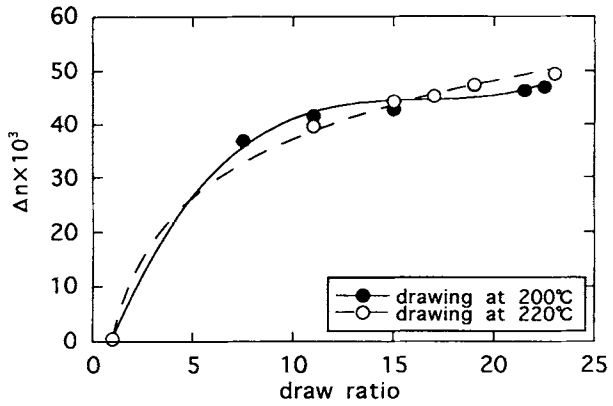

Figure 8 Dependencies of the birefringence on the draw ratio: (●) drawing at 200°C; (○) drawing at 220°C.

was over 50%. It seems that water and PVA competitively add to NMMO and the addition of water to NMMO is superior to that of PVA to NMMO. In other words, NMMO adds to water exclusively and the complex consisting of water and NMMO does not influence the dissolution of PVA. In short, the interaction energy between NMMO and PVA molecules is smaller than that between NMMO and water, i.e., 6 kJ/mol.[13] The s-PVA is difficult to dissolve into water in comparison with a-PVA due to the larger hydrogen bond energy per base mole and dissolves at temperatures above 100°C, whereas it dissolves at temperatures below 100°C in NMMO solution above concentrations of 50% NMMO due to the interaction energy between NMMO and PVA. The spinning of s-PVA was carried out using 70% NMMO solution as a solvent, because the solution is the best for the dissolution ability of PVA.

Figures 2 and 3 show the gelation ability of each PVA solution. The solution containing about 30% NMMO formed a gel very easily, while for the solutions containing over 30% NMMO, it was very difficult to form a gel as the NMMO concentration increased. In the solution containing 30% NMMO, gelation was accelerated, because water or NMMO participating in the dissolution of PVA was the least at this concentration. In other words, PVA dissolves through water in the solutions containing 30% NMMO and NMMO in the solutions containing over 30% NMMO. The complex consisting of PVA and NMMO seems to prevent hydrogen bonds from forming between the PVA chains. The syndiotacticity of PVA remarkably influenced the gelation. In a-PVA solutions, the concentration ranges of polymer and NMMO to make gels were narrower than those of s-PVA solutions at −34°C. No gelation occurred at 0°C in the concentration range of polymer and NMMO in which the s-PVA solutions gelled. Although these mixed solvents have a gelation ability similar to other solvents, the gelation temperature is lower and the handling of solution is better than that of other solvents.

The Mark–Houwink–Sakurada equation,

$$[\eta] = KM^{\alpha}$$

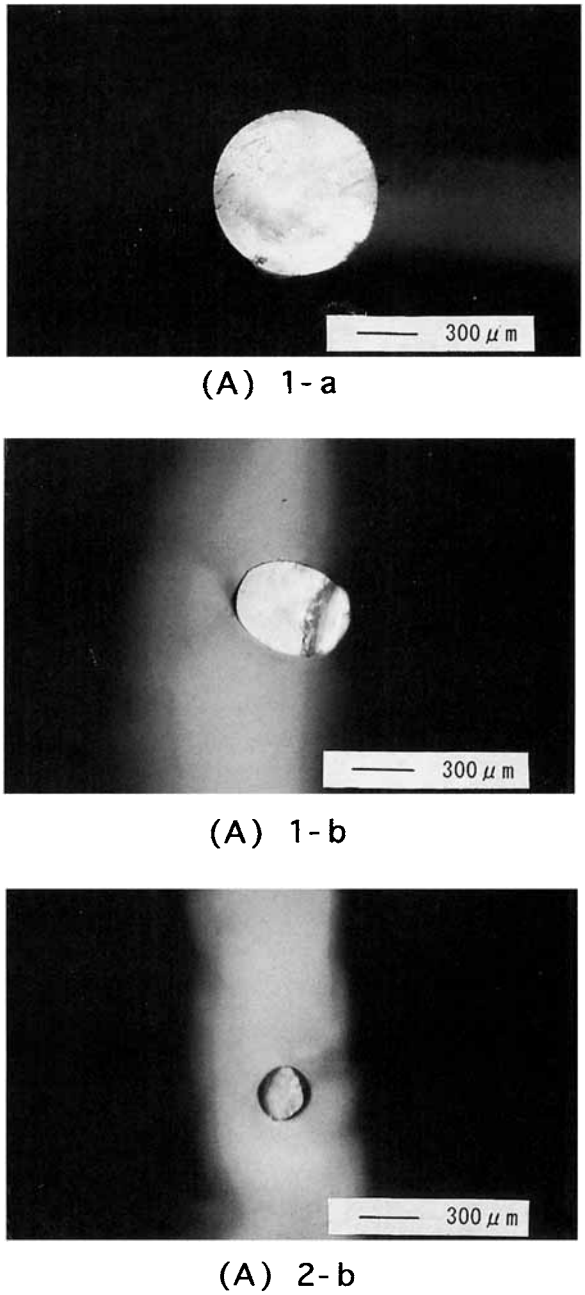

Figure 9 POM micrographs of PVA fibers: (A) cross sections; (B) perspective views.

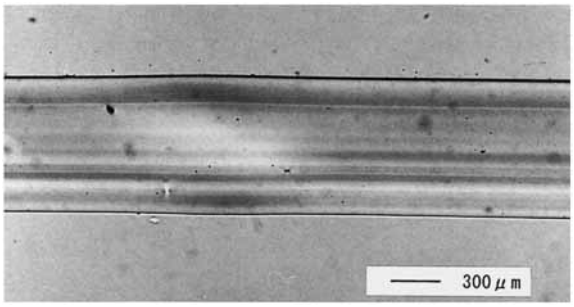

(B) 1-a undrawn fiber

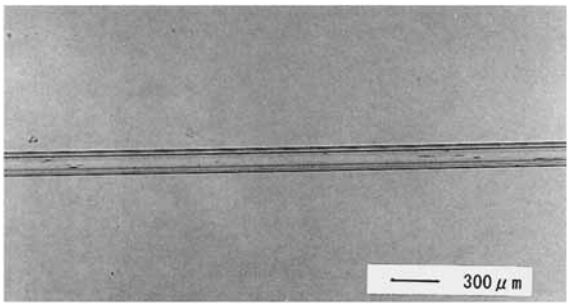

(B) 1-a low-drawn fiber (15 times)

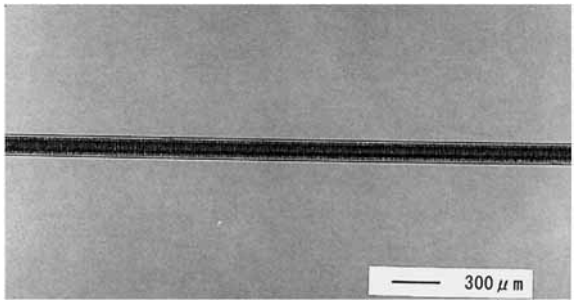

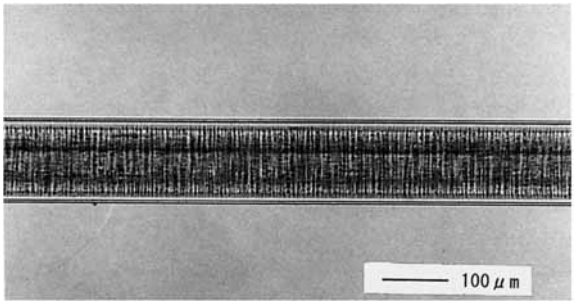

(B) 1-a high-drawn fiber (21.5 times)

Figure 9 (*Continued from the previous page*)

was established where K and α are constants depending on the solvent and temperature. The constant α for the NMMO/water solvent system was estimated from the following equation for the two kinds of PVAs with different molecular weights, where A and B denote polymers A and B:

$$\alpha = \frac{\log([\eta]_A/[\eta]_B)}{\log(M_A/M_B)}$$

By using the intrinsic viscosities of polymers A and B, the α values on a-PVA and s-PVA were calculated to be 0.76 and 0.75, respectively (Table II). The NMMO solution containing 70% NMMO is a good solvent for PVA because the α values are over 0.5. The number of scissions of a polymer S on standing of the solution at 100°C was estimated using $[\eta]_t$ after time t. The relationship between $[\eta]$ and S was reported by Sakurada and Okamura as follows[14]:

1. When the viscosity equation by Staudinger $[\eta] = KM$ is realized,

$$\frac{1}{m} = \frac{2}{S^2}\left(S - 1 + \frac{1}{e^s}\right)$$

2. When $[\eta] = KM^2$ is realized,

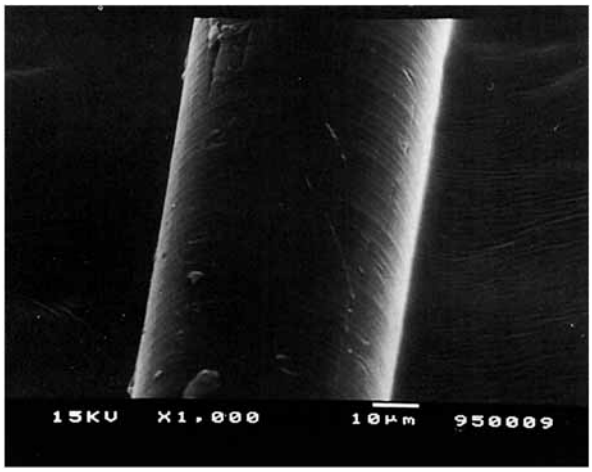

Figure 10 SEM micrograph of the surface of gel-spun PVA fiber drawn until just before breaking.

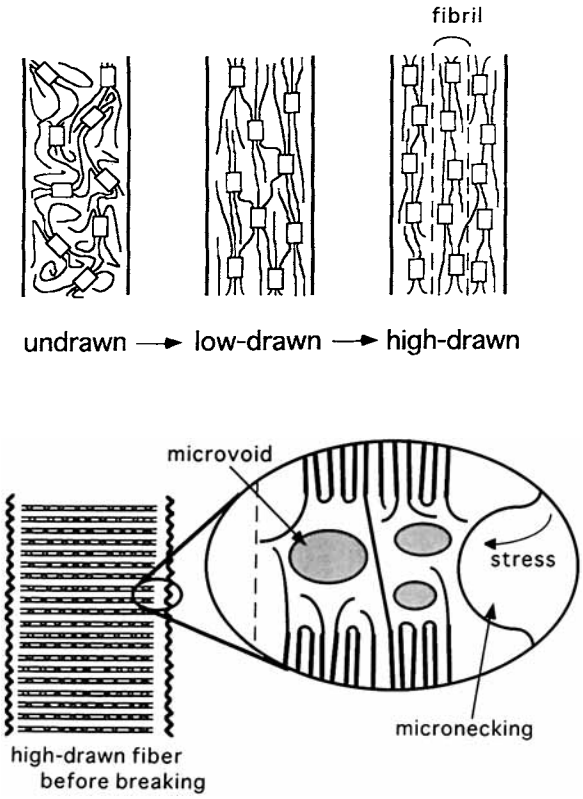

Figure 11 A model of band formation.

$$\frac{1}{m} = \frac{1}{S^2}\left(6S - 12 + \frac{12 + 6S}{e^S}\right)$$

where m is the ratio $[\eta]_0/[\eta]_t$. When the relationship between m and α is graphically drawn for various S values, S is estimated from m in the case of $\alpha = 0.75$. The degree of polymerization after t is as follows:

$$P_t = P_0/(1 + S)$$

Figure 4 shows the change of m with time as $m_0 = 1$ assuming that the reduced viscosities are equal to $[\eta]$. As shown in this figure, the change in solution viscosity with time was quite different in the presence and absence of a stabilizer, and the coloring of the solutions was also different. The scission numbers and the degree of polymerization after 9 h for s(64)-PVA were 0.3 and 950 in the presence of the stabilizer and 1.1 and 520 in the absence of the stabilizer, respectively. The effect of the stabilizer on preventing the breaking of polymer chains is recognized.

The viscosities of PVA/NMMO solutions at different temperatures are shown in Figure 5. Since the viscosity of the spinning solution to prepare commercial PVA fiber is 2500 cps, the spinning temperature was fixed to 80°C, at which the solution had a similar viscosity. The viscosity of the NMMO solution as a solvent is higher than that of water at the same temperature.

The spinning conditions and results are shown in Table III. Table III shows that s(64)-PVA fibers could be spun from the solution with a polymer concentration of 8% through the gel and wet spinning, s(61)-PVA-1 fiber could be spun only with wet spinning from the solution containing s(61)-PVA-1 of 8%, and a-PVA-1 fiber could not be spun through the conditions shown in Table III. The thickness and uniformity of the fiber spun with water was different from those spun with methanol. The fiber prepared by cold water was thick and had a uniform structure, whereas that prepared from methanol was thin and had a heterogeneous skin–core structure. The former is explained by the fiber formation through uniform gelation, while the latter is explained by the coagulation power of methanol.

Figure 6 shows the relationship between draw ratio and tensile strength. The tensile strength tended to increase with draw ratio for every fiber. In the s(64)-PVA, the tensile strength of the fiber gel-spun and drawn at 200°C reached 2.0 GPa. Since the strength of the gel-spun fiber is the highest, the gelation seemed to reduce the entanglements of the polymer chains. The fiber with the highest tensile strength was obtained by drawing at 200°C in this study. However, the highest tensile strength (2.5 GPa) was obtained from the fiber drawn at 220°C in another report.[8] Thus, the relationship between drawing temperature and tensile strength has not yet been clarified. The relationship between the draw ratio and the Young's modulus has a similar influence on the tensile strength.

In Figure 7, the relationships between draw ratio and melting temperature are shown for the fibers prepared by drawing sample 1 – a at 200 and 220°C. The melting point rapidly increased with draw ratio, reaching a value of 267.1°C at the draw ratio of 21.5 for a fiber drawn at 220°C. The value is the highest among all reports about PVA fiber. This is due to the effect of the high syndiotacticity of s(64)-PVA. The heat of fusion of the fibers showed a similar dependence on the draw ratio as did the melting temperature. The heat of fusion rapidly increased with the draw ratio, reaching a value of 6.31 kJ/mol at the draw ratio of 19 for the fiber drawn at 200°C. This corresponds to a crystallinity of 92.3% if based on a value of 6.86 kJ/mol for fully crystalline PVA.

The crystallites in the fiber drawn at 200°C are considered more than that drawn at 220°C.

Figure 8 shows the relationship between the birefringence and draw ratio. The birefringence tended to increase with draw ratio similar to the mechanical properties, except those at high draw ratios, at which it was nearly constant. The birefringence reached 49.5×10^{-3}, a value quite close to the intrinsic birefringence of a fully oriented crystalline PVA. Since the birefringence of PVA fibers drawn at 220°C increased linearly with the draw ratio and was higher than that drawn at 200°C, the entanglement of the polymer chains seemed to be loosened and the PVA crystallites seem to melt in the fiber at the same time. Since the birefringence of an undrawn fiber was nearly equal to zero, the s-PVA molecules in the undrawn fiber are not oriented. This suggests that no orientation during spinning followed by drying occurs.

Figure 9 shows the POM micrograph of PVA fibers drawn at various draw ratios. As stated above, the wet-spinning filament has a transformed cross section, whereas the filament prepared by gel-spinning is uniform and the cross section is close to a genuine circle. Bands were observed in the fibers drawn until just before breaking. Takahashi et al.[15] reported the banded structure of gel-drawn PVA fibers which is similar to the band observed in this study, which was caused by contraction during stress relaxation and interpreted by the model in which the molecular axis is kinked from band to band. However, the band in this study is quite different from the banded structure.

These bands consist of the interior band observed as clusters of black spots in the fiber and the surface band observed as a groove on the surface of the fiber. This surface band also could be observed in the SEM micrograph as shown in Figure 10. The mechanism of the appearance of the bands is considered by the model shown in Figure 11. Micronecking is first formed on the surface of the fiber, and the stress is concentrated on part of the groove. Tie molecular chains in the amorphous regions of the microfibrils are then gradually broken by the concentrated stress. In the amorphous region, the spaces among hair molecular chains, broken tie molecular chains, and folded molecular chains produce microvoids due to the growth by drawing. These microvoids are generally called craze and periodically appear due to the periodic structure of the microfibrils. Since the highest tensile strength in this study or other reports could not determine intrinsic tensile strengths, the cross section of fibers seem to be estimated to be larger than the actual cross section due to these microvoids and microneckings. Tensile strength depends on tie molecular chains and the Young's modulus depends on the orientation of the molecular chains in the amorphous regions. Thus, the magnitude of tacticity is not directly related to the mechanical properties because the amorphous structure is independent of tacticity.

CONCLUSION

s-PVA easily dissolved into highly concentrated NMMO aqueous solution at lower temperatures compared to other solvents. It was difficult to form gels from the PVA solutions. The dissolution is explained by the formation of a complex consisting of NMMO and PVA due to hydrogen bonds between the hydroxyl groups of PVA and the reactive oxygen of NMMO. The NMMO solutions are regarded as good solvents for s-PVA from the calculation results about constant α in the Mark–Houwink–Sakurada equation. It is possible to spin s-PVA fibers from the PVA/NMMO solution using methanol or cold water as the coagulation bath. The gel-spun fibers prepared by extruding the solution into cold water had a uniform structure. The fibers with the highest strength of 2.0 GPa, the highest modulus of 45 GPa, and the highest melting point of 267.1°C were prepared from gel-spun s(64)-PVA fibers. Since these mechanical properties could not provide an intrinsic value, the cross section of the fiber is estimated to be larger than the actual cross section due to microvoids and microneckings. Stopping the formation of microvoids is essential for the enhancement of these mechanical properties.

The authors would like to thank Nihon-nyukazai Co., Ltd., and Kuraray Co., Ltd., for supplying the NMMO and PVAs, respectively.

REFERENCES

1. P. Smith and P. J. Lemstra, *J. Mater. Sci.*, **15**, 505 (1980).
2. H. Fujiwara, M. Shibayama, J. H. Chen, and S. Nomura, *J. Appl. Polym. Sci.*, **37**, 1403 (1989).
3. K.-S. Hwang, C.-A. Lin, and C.-H. Lin, *J. Appl. Polym. Sci.*, **52**, 1181 (1994).
4. R. Schellkens and C. Bastiaansen, *J. Appl. Polym. Sci.*, **43**, 2311 (1991).

5. W.-I. Cha, S.-H. Hyon, and Y. Ikada, *J. Polym. Sci. Polym. Phys. Ed.*, **32,** 297 (1994).
6. T. Kunugi, T. Kawasumi, and T. Ito, *J. Appl. Polym. Sci.*, **42,** 2101 (1990).
7. S. Matsuzawa, L. Sun, and K. Yamaura, *Koubunshi Ronbunsyu,* **48,** 691 (1991).
8. M. Okazaki, N. Miyasaka, and S. Matsuzawa, *Koubunshi Ronbunsyu,* **52,** 711 (1995).
9. Y. Go, S. Matsuzawa, and K. Nakamura, *Kobunshi Kagaku,* **25,** 62 (1968).
10. K. Yamaura, K. Hirata, S. Tamura, and S. Matsuzawa, *J. Polym. Sci. Polym. Phys. Ed.*, **23,** 1703 (1986).
11. S. M. Hudson and J. A. Cucuo, *J. Macromol. Sci. Rev. Macromol. Chem. C,* **18,** 1 (1980).
12. S. Matsuzawa, K. Yamaura, S. Yamada, Y. Shinke, Y. Nakano, and Y. Koike, *J. Appl. Polym. Sci.*, **35,** 391 (1988).
13. A. V. Yakimanskii, A. M. Bochek, V. A. Zubkov, and G. A. Petropavlovskii, *Zh. Prikl. Khim.*, **64,** 622 (1991).
14. I. Sakurada and S. Okamura, *Kogyokagaku Zasshi,* **45,** 1101 (1942).
15. T. Takahashi, K. Suzuki, T. Aoki, and K. Sakurai, *J. Macromol. Sci.—Phys.*, **B30,** 101 (1991).

Received February 9, 1996
Accepted June 1, 1996